
NON-LINEAR REGRESSION MODELS FOR BEHAVIORAL AND NEURAL DATA ANALYSIS

Vincent Adam
PROWLER.io
Cambridge, UK
vincent.adam@prowler.io

Alexandre Hyafil
Centre de Recerca Matemàtica
Campus UAB Edifici C, 08193 Bellaterra, Spain
and Center for Brain and Cognition
Universitat Pompeu Fabra, 08018 Barcelona, Spain

ABSTRACT

Regression models are popular tools in empirical sciences to infer the influence of a set of variables onto a dependent variable given an experimental dataset. In neuroscience and cognitive psychology, Generalized Linear Models (GLMs) -including linear regression, logistic regression, and Poisson GLM- is the regression model of choice to study the factors that drive participant's choices, reaction times and neural activations. These methods are however limited as they only capture linear contributions of each regressors. Here, we introduce an extension of GLMs called Generalized Unrestricted Models (GUMs), which allows to infer a much richer set of contributions of the regressors to the dependent variable, including possible interactions between the regressors. In a GUM, each regressor is passed through a linear or nonlinear function, and the contribution of the different resulting transformed regressors can be summed or multiplied to generate a predictor for the dependent variable. We propose a Bayesian treatment of these models in which we endow functions with Gaussian Process priors, and we present two methods to compute a posterior over the functions given a dataset: the Laplace method and a sparse variational approach, which scales better for large dataset. For each method, we assess the quality of the model estimation and we detail how the hyperparameters (defining for example the expected smoothness of the function) can be fitted. Finally, we illustrate the power of the method on a behavioral dataset where subjects reported the average perceived orientation of a series of gratings. The method allows to recover the mapping of the grating angle onto perceptual evidence for each subject, as well as the impact of the grating based on its position. Overall, GUMs provides a very rich and flexible framework to run nonlinear regression analysis in neuroscience, psychology, and beyond.

Keywords regression · Gaussian process · neuroscience

1 Introduction

1.1 Regression models for data analysis

Research questions in neuroscience and cognitive science often imply to empirically assess the factors that determine an observed neural activity or behavior in controlled experimental environments. Exploratory analyses on such datasets are typically performed using regression analyses - where the measured data (e.g. neural spike count, subject choice, pupil dilation) is regressed against a series of factors (sensory stimuli, experimental conditions, history of neural spiking or subject choices, etc.).

A method of choice is the use of generalized linear models (GLMs [1]) where the dependent variable is predicted from a linear combination of the factors. More formally, GLMs are regression models from the input space \mathcal{X} to the output space \mathcal{Y} specifying a conditional distribution for the variable $y \in \mathcal{Y}$ given a linear projection $\rho(x) = \mathbf{w}^\top \mathbf{x}$ of the input $x \in \mathcal{X}$. ρ is called the predictor. The distribution of $y|\rho(x)$ is chosen to be in the exponential family.

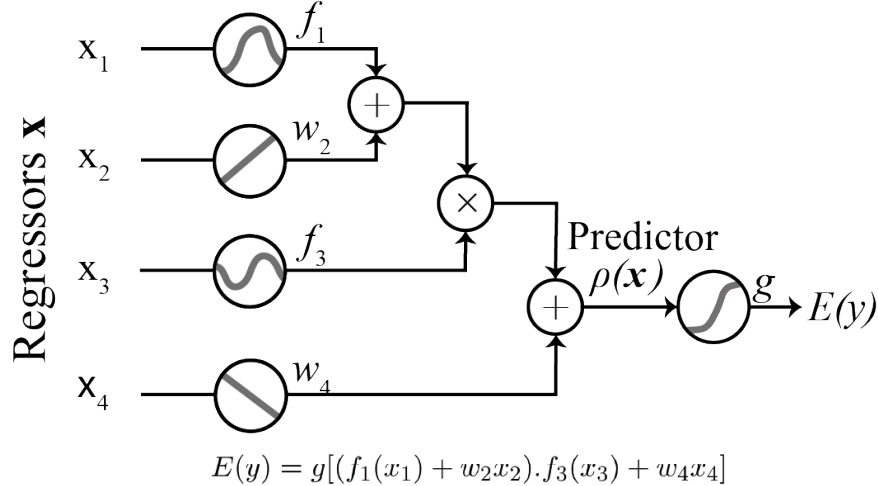


Figure 1: Example of GUM. Here 4 regressors (x_1, x_2, x_3, x_4) are combined to generate a prediction for dependent variable y . Each regressor is first passed through a linear function $w_i x_i$ or non-linear function $f_i(x_i)$. Then regressors are combined with a set of additions and multiplications to yield the predictor $\rho(\mathbf{x})$, in this example $\rho(\mathbf{x}) = (f_1(x_1) + w_2x_2)f_3(x_3) + w_4x_4$. Finally, the expectation for dependent variable $E(y)$ is computed by passing the predictor through a fixed function g (the inverse link function). Inference corresponds to estimating the set of function (\mathbf{w}, \mathbf{f}) based on a dataset (\mathbf{X}, \mathbf{y}) .

This includes, for example, the Bernoulli, the Gaussian and the Poisson distribution that are used to deal with binary, continuous and count data respectively. GLMs are very popular tools due to their good estimation properties (the optimisation problem is convex and iterative estimation procedures converges rapidly), its ease of application and the fact that it can accommodate for many types of data (binary, categorical, continuous) both for regressor and dependent variable. The magnitude of the weight \mathbf{w} is interpreted as indicating the impact of the corresponding factor on the observed data, with a value of 0 indicating an absence of impact.

However, GLMs are intrinsically limited by their underlying assumption that the predictor linearly depends on the regressors. In most situations, we expect regressors to have some non-linear impact onto the neural activity or behavior. Generalized Additive Models (GAMs) are a non-linear extension of GLMs where the linear predictor is replaced by an additive predictor $\rho(x) = \sum_k f_k(x)$ where f_k are functions from $\mathcal{X} \rightarrow \mathcal{Y}$. Each f_k usually depends on one or a subset of dimensions $s_k \subset [1..dim(\mathcal{X})]$ of x (we will make this implicit in the rest of the article by using $f_k(x)$ instead of $f_k(x_{s_k})$). Functions f_k need to be constrained to have some quantifiable form of regularity (e.g. to be smooth), both to make the problem identifiable and to capture a priori assumptions about these functions. Additivity in GAMs introduces another form of identifiability, as functions are only defined up to an offset (i.e. replacing f_1 by $f_1 + \lambda$ and f_2 by $f_2 - \lambda$ for any $\lambda \in \mathbb{R}$ does not change the model). For this reason, it is convenient to add one constraint on each function (i.e. $f_i(0) = 0$) and model the shift factor as an extra parameter $c \in \mathbb{R}$ to be estimated: $\rho(x) = \sum_k f_k(x) + c$.

GAMs release the linearity constraint from GLMs that regressors are mapped linearly onto the predictor. However, one may want to go beyond the additivity hypothesis and allow for non-linear interactions across the variables in the regressor.

1.2 Generalized Unrestricted Model (GUM)

One way to achieve is to extend GAMs and *add* terms that are multiplications of functions to be learned. For example, we would like to capture models such as $\rho(x) = f_1(x)f_2(x) + c$, $\rho(x) = (f_1(x) + f_2(x))f_3(x) + c$, $\rho(x) = f_1(x)f_2(x) + f_3(x) + c$ or $\rho(x) = \sum_i f_1(x_i)f_2(x_i)f_3(x_i) + c$. We define a Generalized Unrestricted Model (GUM) as a regression model composed of the following features: a set of functions or components f_k defined over the input space; a predictor function $\rho(\mathbf{x})$ composed by summations and multiplications of the components; an observation model $y|\rho$ in the exponential family (Figure 1).

The predictor can be constructed recursively using summations and multiplications over the functions. We will study here a relatively general form, where the predictor is a sum of products of sums of GAM predictors (Figure 1):

$$\rho(x) = \sum_i \prod_{j \leq D_i} \left(\sum_l f_{k(ijl)}(x) \right) \quad (1)$$

All of the predictors presented in the previous section can be expressed in such form. As for GLMs and GAMs, GUM regression consists in estimating the components f_k given a dataset of regressor $\mathbf{X} = (\mathbf{x}^{(1)}, \dots, \mathbf{x}^{(N)})$ and a corresponding output $\mathbf{y} = (y^{(1)}, \dots, y^{(N)})$. We refer to a factor as a sum of functions $(\sum_l f_{k(ijl)}(x))$, and to a block as the product of factors. The predictor is thus built as a sum of blocks. The dimensionality of each block D_i is the number of products within the block, i.e. the dimension of the multilinearity. A GAM can be seen as a GUM where all the blocks have dimensionality 1.

1.3 Identifiability of GUMs

Using such a large class of models requires great care to ensure model identifiability. The summation of functions induces a shifting degeneracy, while the multiplication of functions induces a scaling degeneracy:

$$f_1(x)f_2(x) = \frac{f_1(x)}{\lambda}(\lambda f_2(x))$$

for any $\lambda \neq 0$. A general solution to this problem is to constrain all the functions to verify $f_{k(ijl)}(x_0) = 0$ for some given x_0 and to then add offsets $c_{ij} \in \mathbb{R}$ to the model, defining now $\rho(x) = \sum_i \prod_j (\sum_l f_{k(ijl)}(x) + c_{ij}) + c_0$. Equivalently, functions can be constrained to have mean 1 over a certain set of values. We add some further constraints on the offset depending on the model itself (see details in Appendix A). The examples of models provided above will write as: $\rho(x) = (f_1(x) + c_{11})(f_2(x) + 1) + c_0$, $\rho(x) = (f_1(x) + f_2(x) + c_{11})(f_3(x) + 1) + c_0$ or $\rho(x) = (f_1(x) + c_{11})(f_2(x) + 1) + f_3(x) + c_0$.

1.4 Bayesian treatment of GUMs

Recent progress in Bayesian statistics allows to derive algorithms to perform inference in such models that are both accurate and scalable, meaning that they can be efficiently applied to the large datasets produced in neuroscience today. Adopting the framework of probabilistic modelling [2, 3], we frame the model fitting task as probabilistic inference and learning problems. To do so we treat the functions and parameters of the model as latent variables and encode our *a priori* assumptions about these in the form of distributions (using Gaussian processes as priors over functions [4]). Hyperparameters control the statistical properties of the functions, for example their smoothness or periodicity. Inference refers to estimating the functions f and offsets c of the model for a given value of the hyperparameters, while learning refers to estimating the hyperparameters. Due to the model structure, the inference problem is intractable and we resort to an approximate Bayesian inference technique called variational inference [5].

The remainder of this paper is structured as follows. Section 2 reviews the relevant background related to Gaussian process inference and previous work in sparse approximations to GP models. In Section 3 the core methodology for GUMs is presented. Implementation details and computational complexity of the method are covered in Section 4. Section 5 is dedicated to a set of illustrative toy examples and a number of empirical experiments, where practical aspects of GUM inference are demonstrated. Finally, we conclude the paper with a discussion in Section 7.

2 Methods

2.1 Probabilistic modelling and inference

2.1.1 General framework

We propose to tackle the problem of learning the functions and parameters of our regression models as probabilistic inference problems. To do so we start by defining a joint distribution over the dependent variable \mathbf{y} , and the parameters $\boldsymbol{\theta}$ given the regressors \mathbf{x} , with density: $p(\mathbf{y}, \boldsymbol{\theta} | \mathbf{x}) = p(\mathbf{y} | \rho_{\boldsymbol{\theta}}(\mathbf{x}))p(\boldsymbol{\theta})$, where the first term is the exponential family observation model inherited from the GLMs and $p(\boldsymbol{\theta})$ is an *a priori* distribution over the parameters capturing our statistical beliefs or assumptions about their values. In the case of GUMs, parameters correspond to functions and constraints, $\boldsymbol{\theta} = \{f_k, c_k\}$. Both the prior and likelihood may be parameterised by hyperparameters γ . As is the case in most regression models, we will assume that conditioned on the parameters, the observations are statistically independent, i.e. the likelihood factorizes across the data points: $p(\mathbf{y} | \boldsymbol{\theta}) = \prod_n p(y^{(n)} | \boldsymbol{\theta}_n)$, where $\boldsymbol{\theta}_n \subseteq \boldsymbol{\theta}$ is the

subset of parameters on which observation $y^{(n)}$ depends.

We then propose to treat the inference problem as that of computing the *posterior* distribution over the parameters which is defined as their conditional distribution given the observed data $p(\boldsymbol{\theta}|\mathbf{y})$. The posterior density can be expressed using Bayes' rule as $p(\boldsymbol{\theta}|\mathbf{y}) = \frac{p(\mathbf{y}|\boldsymbol{\theta})p(\boldsymbol{\theta})}{p(\mathbf{y})}$. In this expression, $p(\mathbf{y}) = \int p(\mathbf{y}, \boldsymbol{\theta})d\boldsymbol{\theta}$ is the marginal likelihood which is commonly used as a objective to select the value of the hyperparameters γ).

2.1.2 Gaussian processes: distributions over functions

Gaussian processes are commonly used as prior over functions [4] because they can flexibly constrain the space of acceptable solutions in non-linear regression problems. Formally, Gaussian processes are infinite collections of random variables, any finite subset of which follows a multivariate normal (MVN) distribution. They are defined by a mean function m and covariance function k . A sample from a GP defined on an index set X is a function on the domain \mathcal{X} . Given a list of points $X \in \mathcal{X}^N$ and a GP sample $f \sim GP(m, k)$, the vector of function evaluations $f(X)$ is an associated MVN random variable such that $f(X) \sim \mathcal{N}(m(X), K(X, X))$, where $m(X)$ is a vector of mean function evaluations and $K(X, X)$ is a matrix of all pairwise covariance function evaluations ($K(X, X)_{ij} = k(x_i, x_j)$). The covariance function may depend on some hyperparameters γ (the mean function can be too, although in most applications it is taken to be the zero function). For example, the classical Squared Exponential (SE) covariance function defines covariance for real-valued data $\mathcal{X} = \mathbb{R}^d$ based on two hyperparameters: length scale ℓ (which parametrises the expected smoothness of the function) and variance β^2 (which parameterises the expected magnitude of the function) ($k_{SE}(x, x') = \beta^2 e^{-|x-x'|^2/2\ell^2}$). As such, the covariance and mean functions define soft constraints over the functions $f(X)$ that fulfill two goals: make the functions $f(X)$ identifiable, and formalizing assumptions about the possible forms that $f(X)$ may take (i.e. its smoothness).

2.1.3 Variational inference

Evaluating the posterior density $p(\boldsymbol{\theta}|\mathbf{y})$ and the marginal likelihood $p(\mathbf{y})$ is in general intractable for a GUM. We therefore resort to perform approximate inference and focus on variational inference methods [5]. Variational inference turns the inference problem into an optimisation problem by introducing a variational distribution over the parameters $q(\boldsymbol{\theta})$ and maximising a lower bound $\mathcal{L}(q)$ to the log marginal evidence $\log p(\mathbf{y})$. This lower bound is derived using Jensen's inequality :

$$\log p(\mathbf{y}) = \log \int d\boldsymbol{\theta} \frac{p(\mathbf{y}, \boldsymbol{\theta})}{q(\boldsymbol{\theta})} q(\boldsymbol{\theta}) \geq \int q(\boldsymbol{\theta}) \log \frac{p(\mathbf{y}, \boldsymbol{\theta})}{q(\boldsymbol{\theta})} = \mathcal{L}(q) \quad (2)$$

The lower bound can be rewritten as

$$\mathcal{L}(q) = \sum_n \mathbb{E}_{q(\boldsymbol{\theta}_n)} \log p(y_n | \boldsymbol{\theta}_n) - KL[q(\boldsymbol{\theta})|p(\boldsymbol{\theta})], \quad (3)$$

which is the form favored for actual implementations. The left-hand terms in the sum are the *variational expectations* and require computing an expectation under the marginal distributions $q(\boldsymbol{\theta}_n)$.

The gap in the inequality in Equation 2 can be shown to be $\log p(\mathbf{y}) - \mathcal{L}(q) = KL[q(\boldsymbol{\theta})|p(\boldsymbol{\theta}|\mathbf{y})]$, where KL denotes the Kullback-Leibler divergence between distributions. Hence, as $q(\boldsymbol{\theta})$ gets closer to the true posterior $p(\boldsymbol{\theta}|\mathbf{y})$, the bound gets tighter. In practice, one chooses the class of distribution \mathcal{Q} such that optimising $\mathcal{L}(q)$ for q is tractable. Once optimised, the optimal variational distribution $q^*(\boldsymbol{\theta})$ provides an approximation to the posterior and the bound $\mathcal{L}(q^*)$ provides an approximation to the log marginal likelihood.

The choice of the class \mathcal{Q} is driven by two opposite goals: \mathcal{Q} must be rich enough so that at the optimum, q^* captures most important features of $p(\boldsymbol{\theta}|\mathbf{y})$, but simple enough that $\mathcal{L}(q)$ is computationally efficient to evaluate for all $q \in \mathcal{Q}$. When a finite dimensional parameter $\boldsymbol{\theta}$ is endowed a prior distribution which is a multivariate normal (MVN) distribution, a convenient choice for \mathcal{Q} is the class of MVN distributions parameterised by a mean vection $\boldsymbol{\mu}_q$ and a covariance $\boldsymbol{\Sigma}_q$, i.e. $q(\boldsymbol{\theta}) = \mathcal{N}(\boldsymbol{\theta}; \boldsymbol{\mu}_q, \boldsymbol{\Sigma}_q)$ [6]. In that case, computing the marginals $q(\boldsymbol{\theta}_n)$ is straightforward and the KL between two MVNs has a simple expression. The evaluation of the variational expectations in Equation 3 can be evaluated in closed form or approximated using Gaussian quadrature or Monte Carlo methods [7].

When working with functions $f(\cdot)$ and using Gaussian Processes - infinite dimensional objects - as priors, an efficient and scalable way to parameterise the variational distribution as a finite dimensional Gaussian Process expressed at

some input $z \in \mathcal{X}^M$ as follows:

$$q(f(\cdot), \mathbf{f}) = p(f(\cdot)|f(\mathbf{z}) = \mathbf{f})q(\mathbf{f}),$$

where $\mathbf{f} = f(\mathbf{z})$, $q(\mathbf{f}) = \mathcal{N}(\mathbf{f}; \boldsymbol{\mu}_{\mathbf{f}}, \boldsymbol{\Sigma}_{\mathbf{f}})$ is a MVN distribution and $p(f(\cdot)|f(\mathbf{z}))$ is the conditional prior process. $q(\mathbf{f})$ can be interpreted as an approximate marginal posterior on $f(\mathbf{z})$. Choosing $z = x$ is the classical variational treatment of GPs but leads to a computational cost to evaluate $\mathcal{L}(q)$ that scales cubically with N , making the use of variational inference prohibitively expensive for large datasets. Choosing $z \in \mathcal{X}^M$ to be a set of pseudo-inputs (or *inducing points*) of size M leads to the so-called sparse variational approach [8, 7, 9, 10] whose $\mathcal{O}(NM^2 + M^3)$ complexity allows to scale variational inference with GPs to large datasets.

In order to enforce the necessary constraints that make the model identifiable, it is possible to force the posterior processes to have a predictive mean at an input x_c to be equal to y_c . To do so we adjust the variational mean by a scaled unit vector $\boldsymbol{\mu}_{\mathbf{f}} \leftarrow \boldsymbol{\mu}_{\mathbf{f}} + \delta \mathbf{1}$ such that $\mathbb{E}_q[f(x_c)] = y_c$, where $\delta = \frac{y_c - \mathbb{E}_p[f(x_c)|f(\mathbf{z}) = \boldsymbol{\mu}_{\mathbf{f}}]}{\mathbb{E}_p[f(x_c)|f(\mathbf{z}) = \mathbf{1}]}$. This is the method we use in our examples.

2.1.4 Laplace approximation

The Laplace approximation provides an alternative MVN approximation $q(\boldsymbol{\theta}) = \mathcal{N}(\boldsymbol{\theta}; \boldsymbol{\mu}_q, \boldsymbol{\Sigma}_q)$ to the posterior $p(\boldsymbol{\theta}|\mathbf{y})$. This approximation is derived from a Taylor expansion of the log-joint density $\log p(\boldsymbol{\theta}, \mathbf{y})$ taken at the maximum a posteriori parameters $\boldsymbol{\theta}^{\text{MAP}} = \arg \max_{\boldsymbol{\theta}} p(\boldsymbol{\theta}, \mathbf{y})$:

$$\log p(\boldsymbol{\theta}, \mathbf{y}) \approx a + b(\boldsymbol{\theta} - \boldsymbol{\theta}^{\text{MAP}}) - \frac{1}{2}(\boldsymbol{\theta} - \boldsymbol{\theta}^{\text{MAP}})^T H(\boldsymbol{\theta} - \boldsymbol{\theta}^{\text{MAP}}) \quad (4)$$

where $a = \log p(\boldsymbol{\theta}^{\text{MAP}}, \mathbf{y})$, $b = \nabla_{\boldsymbol{\theta}} \log p(\boldsymbol{\theta}, \mathbf{y})|_{\boldsymbol{\theta} = \boldsymbol{\theta}^{\text{MAP}}} = 0$ by definition of $\boldsymbol{\theta}^{\text{MAP}}$, and $H = -\nabla \nabla_{\boldsymbol{\theta}} \log p(\boldsymbol{\theta}, \mathbf{y})|_{\boldsymbol{\theta} = \boldsymbol{\theta}^{\text{MAP}}}$. H is a definite-positive matrix since it is the opposite Hessian of a function evaluated at its maximum. The expansion leads to

$$p(\boldsymbol{\theta}|\mathbf{y}) \propto p(\boldsymbol{\theta}, \mathbf{y}) \approx e^a \exp\left(-\frac{1}{2}(\boldsymbol{\theta} - \boldsymbol{\theta}^{\text{MAP}})^T H(\boldsymbol{\theta} - \boldsymbol{\theta}^{\text{MAP}})\right) \quad (5)$$

The constant of proportionality is obtained from the normalization constraint $\int p(\boldsymbol{\theta}|\mathbf{y}) d\boldsymbol{\theta} = 1$, yielding the MVN form $p(\boldsymbol{\theta}|\mathbf{y}) = \mathcal{N}(\boldsymbol{\theta}; \boldsymbol{\mu}_q, \boldsymbol{\Sigma}_q)$ with $\boldsymbol{\mu}_q = \boldsymbol{\theta}^{\text{MAP}}$ and $\boldsymbol{\Sigma}_q = H^{-1} = [-\nabla \nabla_{\boldsymbol{\theta}} \log p(\boldsymbol{\theta}, \mathbf{y})|_{\boldsymbol{\theta} = \boldsymbol{\theta}^{\text{MAP}}}]^{-1}$.

The Laplace approximation is a fairly simple procedure, as it only requires to find the maximum a posteriori parameters $\boldsymbol{\theta}^{\text{MAP}}$, and to then compute the Hessian of the log-joint probability evaluated at $\boldsymbol{\theta}^{\text{MAP}}$. The approximation is increasingly better as the sample size n increases, as the true posterior becomes closer to a MVN distribution [3]. However the computational complexity of the method scales cubically with the number of data points.

2.2 Approximate inference for GUMs

We present two different approximate methods to treat GUMs: Laplace approximation and sparse variational inference. For each method, we describe first how inference can be performed, i.e. how the posterior over the functions f and offsets c can be approximated from a dataset, assuming fixed values of the hyperparameters for the different GPs. Then, for each method, we describe how these hyperparameters can also be learned from the dataset.

2.2.1 Laplace approximation for GUMs

Inference For classical GP classification, the Laplace approximation follows by recognizing that the problem is formally equivalent to a Bayesian GLM, where the parameters are the value of the GP at data points $\mathbf{f} = f(\mathbf{x})$, the prior covariance is given by the GP evaluated at data points $K(\mathbf{x}, \mathbf{x})$ and the design matrix is identity [4]. Then the MAP solution \mathbf{f}^{MAP} can be found iteratively using Newton-Raphson updates (the joint density is convex), and the Hessian can be evaluated analytically. Computing the Laplace approximation for GUMs follows a similar path. The derivation is quite lengthy, so we summarize here the main steps (details are provided in Appendix B).

First, a GUM can be turned into a Bayesian formulation of a generalized multilinear model [11, 12], as multiplications of functions yield multilinear interactions of the parameters $\mathbf{f}_k = f_k(\mathbf{x})$. The constraints on f_k added to remove identifiability problems lead to removing one free parameter for each parameter set \mathbf{f}_k . The MAP solution is then found by iteratively performing Newton-Raphson update on each dimension while leaving others parameters unchanged. For example for a GUM $\rho(x) = f_1(x)f_2(x)$, we update the value of \mathbf{f}_1 while leaving \mathbf{f}_2 unchanged, then we update \mathbf{f}_2 while \mathbf{f}_1 is unchanged, and loop until convergence. Each iteration increases the value of the joint density. Finally, the covariance of the approximated posterior can be computed analytically by evaluating the Hessian of the log joint density at the MAP parameters.

Hyperparameter fitting For Laplace approximation we describe two different ways of fitting the hyperparameters γ for the prior covariance functions $\mathbf{K}_{ij} = \mathbf{K}_{ij}(\gamma_{ij})$: cross-validation and generalized expectation-maximisation [13].

In cross-validation, we split the dataset between a training set and a test set (possibly multiple times, as in K-fold cross-validation). We infer the MAP estimate θ^{MAP} using the training set only, then compute the cross-validated log-likelihood (CVLL), i.e. the log-likelihood of the MAP parameters evaluated on the test set $\log p(\mathbf{y}_{\text{test}}|\theta^{\text{MAP}})$. The gradient of the CVLL over the hyperparameters can be calculated analytically (see Appendix B.4.1). This allows to run a gradient ascent algorithm which iterates between computing the MAP estimates for given hyperparameters and then updating the hyperparameters to along the gradient to improve the CVLL score.

In expectation-maximisation, we used the approximated posterior $q(\theta)$ to update the lower bound on model evidence $\mathcal{L}(q, \gamma) = \int q(\theta) \log p(\mathbf{y}|\theta, \gamma) d\theta + \text{const.}$ The algorithm iterates between the expectation step (inference using Laplace approximation) and the maximisation step where the lower bound is maximised with respect to the hyperparameters. Because both priors and posteriors are Gaussian, the lower bound can be expressed analytically and maximised using gradient ascent. Note however that, because the posterior is not exact but approximated, the lower bound is not guaranteed to increase at each expectation step.

2.2.2 Sparse variational approximation for GUMs

Inference Variational inference has been used to learn GLMs [14] and GAMs [15, 16]. In these settings, having multiple functions, we need to specify a variational posterior over the functions and scalar parameters $q(f_{1\dots K}, \mathbf{c})$. We follow [17] and assume it factorizes as

$$q(f_{1\dots K}, \mathbf{c}) = q(\mathbf{f}_{1\dots K}, \mathbf{c}) \prod_k p(f_k | f_k(\mathbf{z}_k) = \mathbf{f}_k),$$

which means that posterior processes are only coupled through the inducing variables $\mathbf{f}_{1\dots K} \in \mathbb{R}^{\sum_k M_k}$ (M_k is the number of inducing points for f_k).

We are left to characterize the finite density $q(\mathbf{f}_{1\dots K}, \mathbf{c})$. We choose to parameterise it as a MVN distribution. A first option is to parameterise it as fully coupled MVN distribution, which would capture the posterior coupling but would also do so in a overparameterised fashion. The other extreme would consist in a mean field approximation across term $q(\mathbf{f}_{1\dots K}, \mathbf{c}) = \prod_k q(\mathbf{f}_k) \prod_i q(c_i)$ which would under-estimate the posterior variances [3] and possibly bias learning [18].

We propose a parameterisation that preserves coupling across functions: $q(\mathbf{f}_{1\dots K}, \mathbf{c}) = q(\mathbf{f}_{1\dots K}) \prod_i q(c_i)$, where we let each factor be a MVN distribution. For each function we enforce $q(f_k(0)) = 0$ using the method described in Section 2.1.3.

Hyperparameter fitting When using variational inference, $\mathcal{L}(q)$ is used as a proxy to the log marginal likelihood and can be optimized with respect to the hyperparameters γ as well as with respect to q , an approach akin to Expectation Maximisation [3]. We here follow this approach: we iterate between maximizing $\mathcal{L}(q)$ over q with γ fixed (inference) and maximizing $\mathcal{L}(q)$ over γ with q fixed (learning).

3 Results

3.1 Synthetic data

We first tested the ability of the different algorithms to infer the correct form of functions from synthetic data. We generated Poisson observations \mathbf{y} ($E(y|\rho) = e^\rho$) from a simple GUM of the form $\rho(\mathbf{x}) = f_1(x_1)f_2(x_2) + f_3(x_3)$ and then applied our algorithms to fit the functions (f_1, f_2, f_3) on the dataset (\mathbf{x}, \mathbf{y}) . We chose f_1 and f_3 to be functions of a closed interval $[0, 2]$ and f_2 to be periodic (of period π). This could correspond for example to regressing the spiking activity of a neuron in visual cortex against the properties of visual stimulus defined by its contrast and orientation: $f_1(x_1)$ would be the modulation of firing rate by contrast, $f_2(x_2)$ the orientation selectivity, and $f_3(x_3)$ could be the fluctuation of neural excitability across time (with x_3 being time). More specifically, we defined $f_1(x_1) = \exp(x_1/2) - 1$, $f_2(x_2) = 1 + \cos(2x_2 + \pi/3)$ and $f_3(x_3) = -\sin(x)$. For estimation of f_1 and f_3 we used the standard Squared Exponential kernel $K_{SE}(x, x') = \beta^2 \exp(-\frac{|x-x'|^2}{2\ell^2})$ with

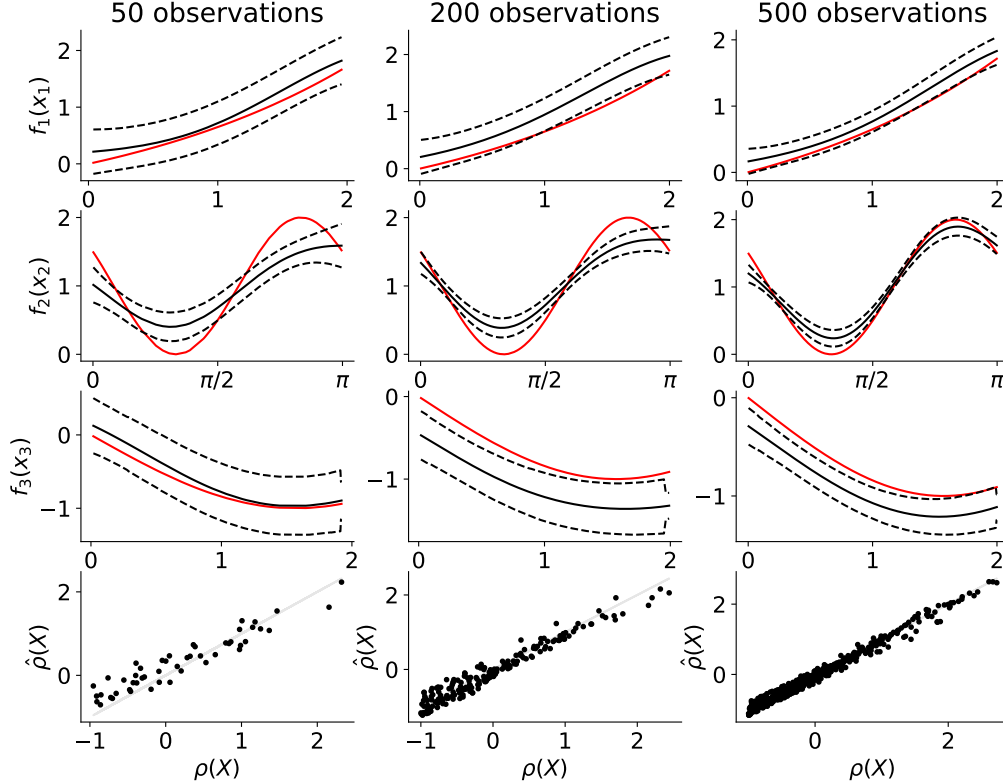


Figure 2: Estimated functions using Laplace method from GUM model with predictor $\rho(x) = f_1(x_1)f_2(x_2) + f_3(x_3)$. Posterior distribution for each function f_i is a Gaussian Process $f_i \sim GP(m_i, k_i)$. Solid black lines depict the posterior mean function $m_i(x)$, dotted lines depict the posterior standard error. Red lines depict the ground truth, i.e. the functions that were used to generate the dataset. Different columns represent different sizes for the dataset used to estimate the functions (50, 200 or 500 observations).

the value of the hyperparameters $\beta = 1$ and length scale $\ell = 0.1$. For f_2 we used the standard periodic kernel $K_{per}(x, x') = \beta^2 \exp(-2 \sin^2(\frac{\pi}{T}|x - x'|)/\ell^2)$, with hyperparameters $\beta = 1$, $\ell = \pi/20$ and period $T = \pi$.

We report the inferred functions and the resulting predictors for both methods in Figure 2 (Laplace method) and Figure 3 (sparse variational inference) which show the functions are correctly recovered, even for small sized. The reconstruction error is compared between the different sizes of the dataset ($N = 50, 200, 500$ observations) in Figure 4. Using priors over the functions implies that the estimator will be biased (towards zero), and that the bias will be larger for smaller datasets. In practice, however, such shrinking effect was very small for $N = 200, 500$, and was only pronounced for the smaller sample size ($N = 50$) for the estimation of f_2 . As expected, all three functions were more accurately estimated for larger sample sizes. Both methods achieve similar regression performance as measured by the root mean squared error (RMSE) on the predictor, which decreases as the number of observations grows (Figure 5). In terms of computing however, the sparse variational method clearly outbeats the Laplace method for large sample size (from $N = 500$). For the Laplace method, we also report the reconstruction error between the true function f_i and estimated function \hat{f}_i as $err_i = \langle (f_i(x_i) - \hat{f}_i(x_i))^2 \rangle_{x_i}$.

3.2 Experiments: psychophysical data - perceptual decision study

The very flexible functional forms of GUMs makes them applicable to a wide range of problems in psychophysics, neuroscience and beyond. We illustrate GUMs on experimental data from a study using a classical evidence accumulation paradigm [19].

A classical problem in cognitive neuroscience is to understand how humans integrate evidence from multiple sources of information to make decisions [19]. One embodiment of this problem is the study of how this integration happens across time given a temporal sequence of stimuli, such as oriented gratings [20]. In such paradigms, subjects report

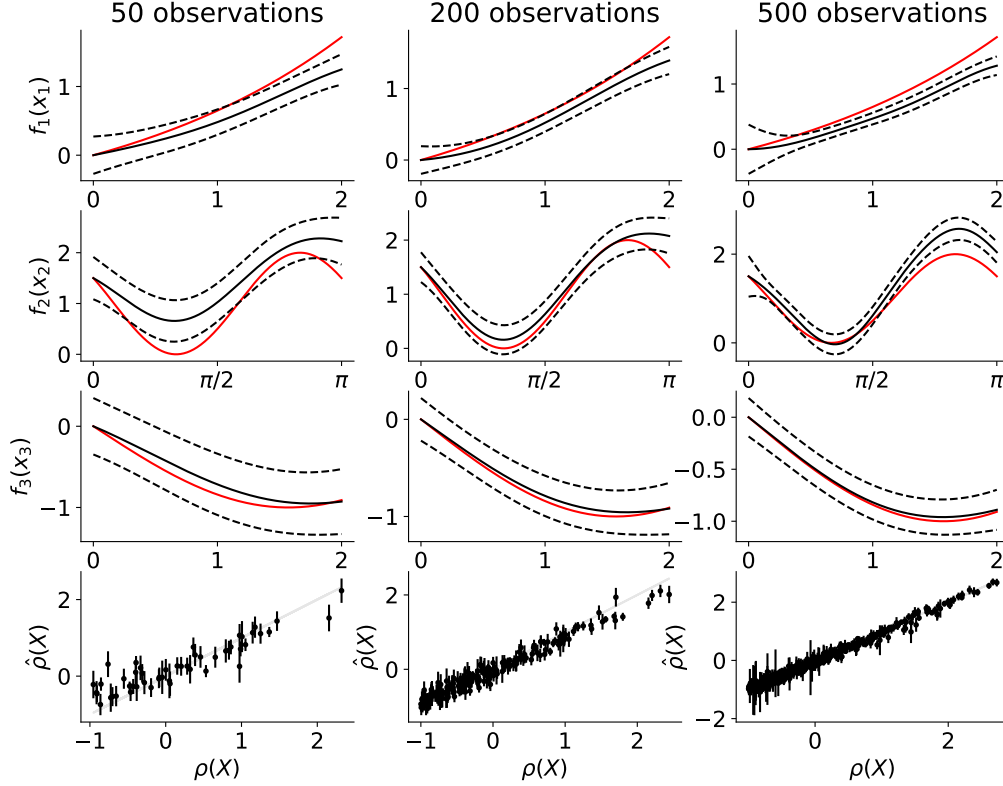


Figure 3: Estimated model using the variational inference for GUM model with predictor $\rho(\mathbf{x}) = f_1(x_1)f_2(x_2) + f_3(x_3)$, for same dataset as figure 2. Top three rows: posterior distribution for each function f_i is a Gaussian Process $f_i \sim GP(m_i, k_i)$. Solid black lines depict the prior mean function $m_i(x)$, dotted lines depict the posterior standard error. Red lines depict the ground truth, i.e. the functions that were used to generate the dataset. Different columns represent different sizes for the dataset used to estimate the functions (50, 200 or 500 observations). Bottom row: posterior predictive predictor $q(\rho)$ against ground truth.

through a binary decision the value of a particular statistic of a stimulus feature across the sequence (e.g. whether gratings are mostly tilted clockwise or counterclockwise, figure 6A).

To model the contribution of the different visually presented gratings x_{tk} (where t denote trial number and k the index of the grating in the sequence) to the behavioral response y_t , a binomial GLM (i.e. logistic or probit regression) is frequently used. Such a model has the form: $p(y_t = 1) = \sigma(\rho)$ and $\rho = \sum_k w_k z_{tk} + c$, where w_k is the weight of the stimulus in position k , c is the lateral bias towards one response and $z_{tk} = f(x_{tk})$ is a (possibly non-linear) transformation defined by the normative framework (formally, $z_{tk} = \log \frac{p(x_{tk}|\hat{y}=1)}{p(x_{tk}|\hat{y}=0)}$). In the grating task task, $z_{tk} = \cos(x_{tk} - \theta_{\text{ref}})$.

3.2.1 Learning a mapping from stimuli to evidence

The GUM framework allows to extend the types of models we can fit beyond this standard GLM, and capture rich interactions between factors to explain behavior. Notably, the mapping f from sensory to perceptual evidence may depart from the normative standpoint. The particular shape of the mapping may depend on how orientation is encoded by neural populations in the visual cortex, or the way the task is presented to the participants. We can formulate a GUM model where such mapping f is learned from data rather than defined *a priori*: $\rho(\mathbf{x}) = \sum_k w_k f(x_{tk}) + w_0$. This model relies on the multiplicative interaction between the stimulus weights w_k and the non-linear mapping f , one defining feature of GUMs. This GUM is related to a strictly additive model (GAM) $\rho(\mathbf{x}) = \sum_k f_k(x_{tk}) + w_0$ where one stimulus mapping f_k is defined for each position in the sequence. However this latter model ignores the fact that all stimuli are similar in nature and processed by the same sensory areas, so that the mapping should be conserved up to a scaling factor. Adding the scaling constraint $f_k(x) = w_k f(x)$ gives the GUM equation, a model with better interpretability and with less parameters (a single mapping function to be fitted), so that it can be inferred

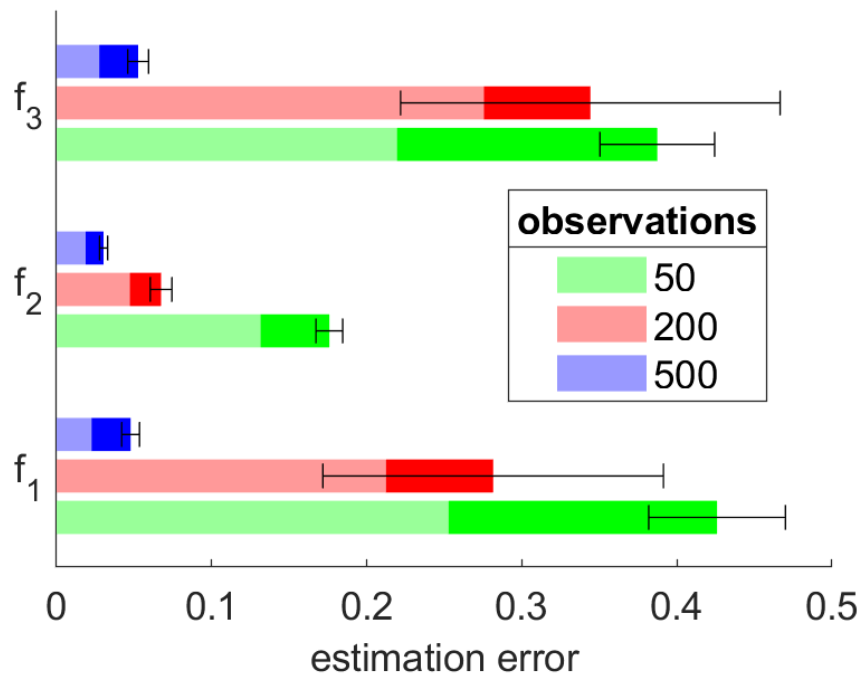


Figure 4: Estimation error for functions f_1 , f_2 and f_3 in GUM with predictor $\rho(\mathbf{x}) = f_1(x_1)f_2(x_2) + f_3(x_3)$, as a function of the number of observations. Values represent the average expected error over 30 repetitions of GUM inference (as in Figure 2). Error bars represent the s.e.m. Lighter bar represents the proportion of the due due to error in posterior mean, while darker portion represents the proportion due to posterior variance (see C for details).

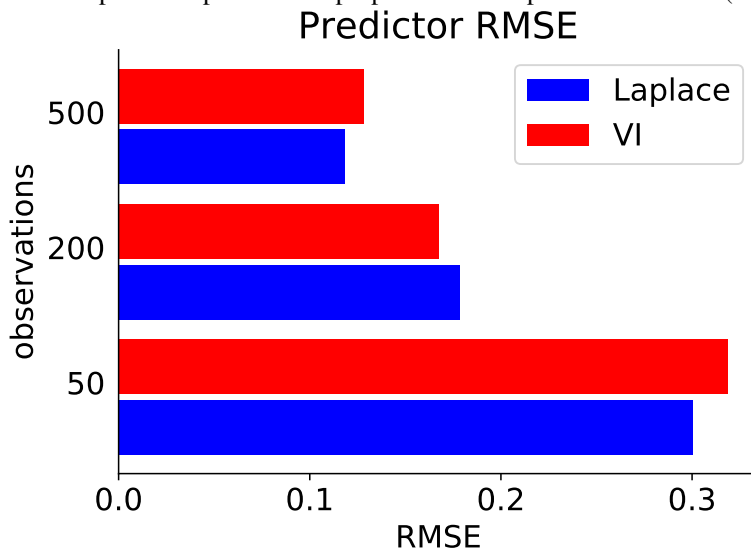


Figure 5: Root Mean Squared Error (RMSE) of the posterior predictor against ground truth for both the Laplace and the Variational inference methods.

precisely with less observations.

We estimated the GUM model above on choice data from 9 participants that each performed 480 trials. We used a GP with periodic covariance function as a prior for f , and the function and its hyperparameters were estimated using the Laplace method with cross-validation. To handle identifiability problem, we constrained the weights to be on average 1 ($\frac{1}{N} \sum_{k=1}^N w_k = 1$). Results are presented for three subjects in Figure 6B-6C. First, different subjects displayed different psychophysical kernels, i.e. different profiles of grating weight w_k . While subject 1 assigned more weight to gratings presented early in the sequence (the so-called *primacy effect*), subject 2 assigned more weight to gratings showed late (*recency effect*), and subject 3 displayed more or less equal weighting for all gratings. These patterns obtained from the GUM matched the profiles obtained from the more traditional GLM analysis. More importantly, the GUM analysis permitted to recover for each subject how each grating was mapped on the decision space based on its angle, i.e. the decision mapping $f(x)$. the mapping of subject 1 is very similar to the cosine function predicted by the normative approach: gratings with relative angle of 0 (i.e. perfectly aligned with the reference grating) provided maximal bias in favor of the associated choice (rightward response), while gratings with relative angle of 90 degrees (i.e. perpendicular to the reference grating) provided maximal bias in favor of the alternative choice (leftward response). The mapping for subject 2 looked similar but with a vertical offset: leftward-tilted gratings provided more bias towards left response than rightward-tilted did towards right response. Finally, mapping for subject 3 showed a much more abrupt transition from angles biasing the decision towards the left to angles biasing towards the right response. This is more consistent with a subject that simply categorizes the gratings as being tilted leftwards or rightwards and bases its decision based on the counts for each category, disregarding the precise angular distance of each grating to the references. It should be noted that GP always enforces a degree of smoothness to the recovered function, so that a step function could not be inferred with a finite dataset.

We performed a model comparison to test, for each participant, whether the GUM provided a better account of the behavioral data than the simpler GLM model. This analysis shows whether using a flexible mapping instead of the fixed normative one (cosine function) improves the model. We used the Akaike Information Criterion, that corrects the approximate marginal evidence $\mathcal{L}(q, \gamma)$ with the number of hyperparameters p ($AIC = 2p - 2 \log \mathcal{L}(q, \gamma)$). The results were in agreement with what we observe for individual mappings (figure 6E). For subject 1, whose mapping was very similar to the normative one, the GLM was favored. For subject 2 and 3, whose mapping differed from the normative one, the GUM was favored. Finally, the fitted values of the hyperparameters provides an information about the degree of smoothness of the mapping that provided the best account of the data. In particular, the values of the length scale for the squared exponential was 4.1 ± 3.1 degrees (average \pm std across participants) (figure 6D).

4 Discussion

Here we have presented a novel class of regression models, Generalized Unrestricted Models or GUMs, that allows to capture nonlinear mapping for each regressor, as well as additional and multiplicative interactions between these regressors. We propose a Bayesian treatment of GUMs using the framework of Gaussian Processes, that allow to define distributions over functions with interpretable properties. Moreover, GUMs allow to perform regression for many different data type (including binary variable, categorical, real, periodic), making it an extremely versatile analysis method.

We have shown two different algorithms to learn GUMs from experimental data: the Laplace method and the sparse variational approach, which scales better for larger dataset. A GUM analysis on synthetic data showed that both methods allowed to recover mappings with low estimation error, even for small datasets. However, we strongly advise to run parameter recovery analysis for any new GUM problem. Indeed the estimation error will largely depend on the class of the model and the size of the dataset. For some classes of models, the identifiability may be poor. Using multiple initial values for the estimation procedure is key to avoid finding local solutions to the estimation problem, but may not always correct this identifiability issue.

There is a long history of using regression analyses that capture multiplicative interactions between regressors. ANOVA is routinely used to capture these interactions for categorical regressors and continuous dependent variable. This is equivalent to defining a GLM that includes multiplication of the regressors into the design matrix (which is the method of choice for non-normally distributed dependent variable). For continuous regressors, previous studies have looked at extensions of the GLM and other regression models to include bilinear or multilinear terms [12, 21, 22, 11, 23]. As in the Laplace method, estimation techniques for such models rely on alternatively updating the weights associated to one dimension while leaving the other weights fixed. However those regression models did not capture multiplication of non-linearly transformed regressors (i.e. $f_1(x)f_2(x)$). One exception is the work of Ahrens and colleagues who built multilinear models of neural spiking activity [22], where each neuron firing rate $r(t)$ is based on spatio-temporal filtering of the acoustic stimuli $S(f, t)$ that is separable in time delay d and frequency f ,

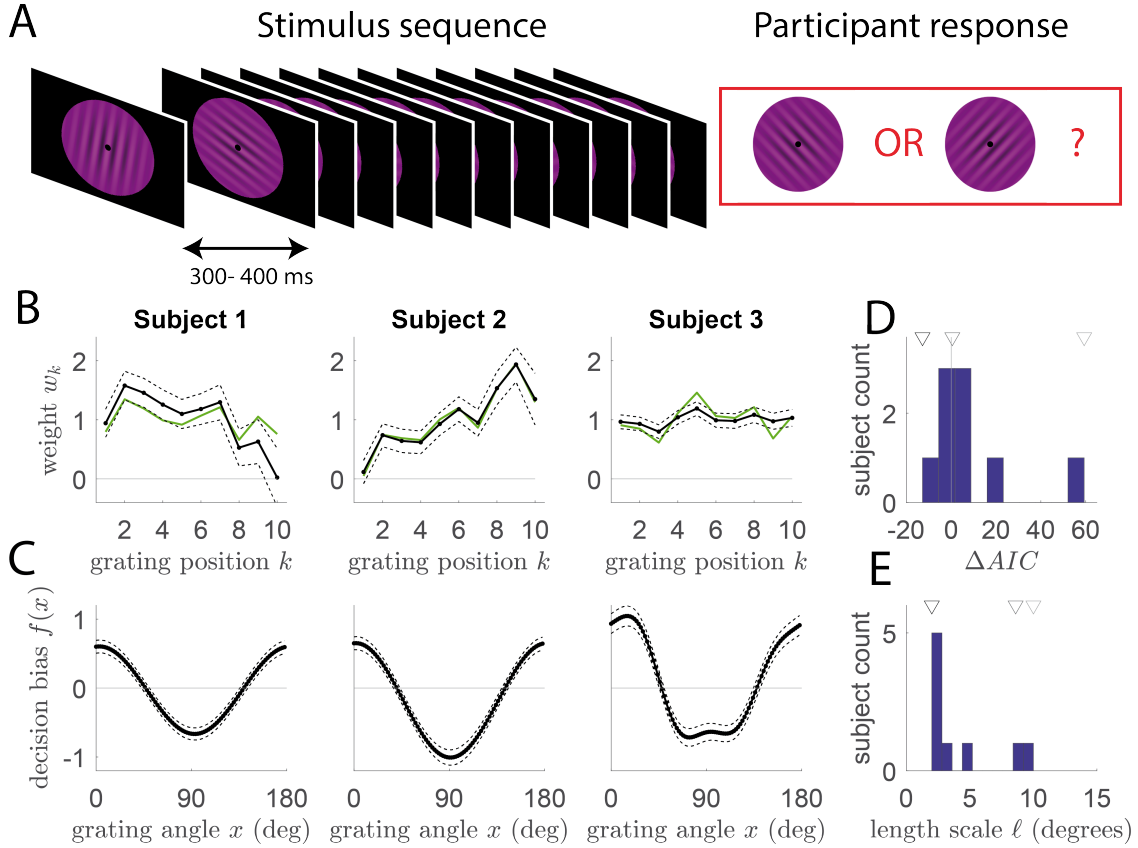


Figure 6: Application of GUM to analysis of human psychophysics experiment **A**. Behavioral paradigm. In each trial, the participant viewed a sequence of 5-10 visual gratings with a certain orientation, interspersed with a 300-400 ms interval. Subjects had to report at the end of the sequence whether the average orientation of the gratings was more tilted clockwise or counter-clockwise. **B**. Psychophysical kernels recovered from the GUM analysis for 3 exemplar subjects. The kernel represents the weight of each grating w_k as a function of its position k in the stimulus sequence. Full black line represents the posterior mean, and dotted black lines the standard deviation, obtained using the Laplace method. The green line represents the weights obtained from the standard GLM analysis. **C**. Perceptual mapping for each subject, i.e. the decision update $f(x)$ for each grating as a function of its orientation x relative to the reference orientation (orientation tilted clockwise, i.e. 45 degrees). Positive (resp. negative) values indicate that the grating biases the decision towards the 'tilted clockwise' (resp. 'tilted counter-clockwise') response. Perceptual mapping were estimated from GUM model, legend as in **B**. **D**. Histogram of difference in Akaike Information Criterion (ΔAIC) between the GUM and simpler GLM, for all 9 participants. Positive values indicate that the GUM is favored, negative that that the GLM is favored. Triangles above indicate values for the 3 subjects of panels B-C (black: subject 1; dark grey: subject 2; light grey: subject 3). **E**. Histogram of fitted values for hyperparameter ℓ that defines the expected length scale of mapping f .

i.e. $E(r(t)) = \sum_{f,d} f_f(f) f_t(d) S(f, t - d)$. GUMs are also related to models designed to infer the latent dynamics of underlying low-dimensional factors from simultaneous spike recordings, such as Gaussian Process Factor Analysis (GPFA)[24] or variational Latent Gaussian Process (vLGP)[25]. For example, the predictor in vLGP for spike count for neuron n at time t is built as: $\rho_{nt} = \sum_k \alpha_{nk} f_k(t) + \sum_u \beta_{nu} y_{n,t-u} + c_n$, where f_k is a collection of latent processes modelled as GPs, α_{nk} represent the weight of latent process k onto each neuron n , β represent the impact of spike history onto neuron firing, and c_n sets the baseline firing rate for neuron n . Spike count y_{nt} is taken from a Poisson distribution with rate $\exp(\rho_{nt})$. This is one possible functional shape of a GUM. One small difference in treatment however is that weights α and β were modelled as hyperparameters rather than latent processes themselves, in other words their solution did not model uncertainty about weight estimation.

In essence, the GUM framework expands the catalogue of models that can be estimated from data by adding multilinearity on top of nonlinear mappings. While it can be used as a purely predictive tool for machine learning applications, its primary development is for inference problems, where we are interested in estimating the nature of the influence of regressors over a certain dependent variable. The versatility of the tool, rather than simply expanding the space of possible predictive models, is meant to be at the service of a research question where interpretability is essential. We have provided an example here for analysis of behavioral data. In this example, the interaction between the functions of grating position and grating angle found a natural interpretation: the weights for grating position w_k represent the impact of the grating depending on its position in the sequence, while the mapping from grating angle $f(x)$ represent how each grating biases the decision in favor of one choice or the other depending on its angle. We believe that many scientific questions in neuroscience and beyond could be explored using this new tool, for example: assessing decomposable spectro-temporal receptive fields from neural recordings [22]; assessing complex cross-frequency coupling in neural signals [26]; assessing how an evoked potential in EEG can be modulated parametrically by an experimental factor [27]; etc. We are currently working on a toolbox to make this new versatile regression tool publicly available for analysis of neural and behavioral datasets.

Acknowledgements

This research was supported by the Spanish Ministry of Economy and Competitiveness together with the European Regional Development Fund (PSI2015-74644-JIN and RYC-2017-23231 to A.H.). The authors would like to thank Isis Albareda for her help with the acquisition of behavioral data, V. Wyart for sharing code for the coding of the experimental paradigm, as well as J.Pillow and M.Aoi for fruitful discussions about the GP framework.

References

- [1] P. McCullagh and J. A. Nelder. *Generalized Linear Models*. Chapman & Hall / CRC, 1989.
- [2] David JC MacKay and David JC Mac Kay. *Information theory, inference and learning algorithms*. Cambridge university press, 2003.
- [3] Christopher M Bishop. *Pattern recognition and machine learning*. Springer Science+ Business Media, 2006.
- [4] Carl Edward Rasmussen and Christopher K. I. Williams. *Gaussian Processes for Machine Learning (Adaptive Computation and Machine Learning)*. The MIT Press, 2005.
- [5] David M Blei, Alp Kucukelbir, and Jon D McAuliffe. Variational inference: A review for statisticians. *Journal of the American statistical Association*, 112(518):859–877, 2017.
- [6] Edward Challis and David Barber. Gaussian kullback-leibler approximate inference. *The Journal of Machine Learning Research*, 14(1):2239–2286, 2013.
- [7] James Hensman, Nicolo Fusi, and Neil D Lawrence. Gaussian processes for big data. *arXiv preprint arXiv:1309.6835*, 2013.
- [8] Michalis Titsias. Variational learning of inducing variables in sparse gaussian processes. In *Artificial Intelligence and Statistics*, pages 567–574, 2009.
- [9] Alexander G de G Matthews, James Hensman, Richard Turner, and Zoubin Ghahramani. On sparse variational methods and the kullback-leibler divergence between stochastic processes. In *Artificial Intelligence and Statistics*, pages 231–239, 2016.
- [10] Matthias Bauer, Mark van der Wilk, and Carl Edward Rasmussen. Understanding probabilistic sparse gaussian process approximations. In *Advances in neural information processing systems*, pages 1533–1541, 2016.
- [11] Jianing V. Shi, Yangyang Xu, and Richard G. Baraniuk. Sparse Bilinear Logistic Regression. pages 1–25, 2014.

- [12] Christoforos Christoforou, Robert Haralick, Paul Sajda, and Lucas C. Parra. Second-Order Bilinear Discriminant Analysis. *Journal of Machine Learning Research*, 11:665–685, 2010.
- [13] Simon N. Wood. Fast stable restricted maximum likelihood and marginal likelihood estimation of semiparametric generalized linear models. *Journal of the Royal Statistical Society: Series B (Statistical Methodology)*, 73(1):3–36, jan 2011.
- [14] Hannes Nickisch and Matthias W. Seeger. Convex variational bayesian inference for large scale generalized linear models. In *Proceedings of the 26th Annual International Conference on Machine Learning, ICML '09*, pages 761–768. ACM, 2009.
- [15] Francis KC Hui, Chong You, Han Lin Shang, and Samuel Müller. Semiparametric regression using variational approximations. *Journal of the American Statistical Association*, pages 1–24, 2019.
- [16] Vincent Adam, James Hensman, and Maneesh Sahani. Scalable transformed additive signal decomposition by non-conjugate gaussian process inference. In *2016 IEEE 26th international workshop on machine learning for signal processing (MLSP)*, pages 1–6. IEEE, 2016.
- [17] Vincent Adam. Structured variational inference for coupled gaussian processes. *arXiv preprint arXiv:1711.01131*, 2017.
- [18] R. E. Turner and M. Sahani. Two problems with variational expectation maximisation for time-series models. In D. Barber, T. Cemgil, and S. Chiappa, editors, *Bayesian Time series models*, chapter 5, pages 109–130. Cambridge University Press, 2011.
- [19] Joshua I. Gold and Michael N. Shadlen. The neural basis of decision making. *Annual review of neuroscience*, 30:535–74, jan 2007.
- [20] Valentin Wyart, Vincent de Gardelle, Jacqueline Scholl, and Christopher Summerfield. Rhythmic Fluctuations in Evidence Accumulation during Decision Making in the Human Brain. *Neuron*, 76(4):847–858, nov 2012.
- [21] Antoine de Falguerolles. Generalized Multiplicative Models. In *COMPSTAT*, pages 143–175. Physica-Verlag HD, Heidelberg, 2012.
- [22] Misha B Ahrens, J. F. Linden, and M. Sahani. Nonlinearities and Contextual Influences in Auditory Cortical Responses Modeled with Multilinear Spectrotemporal Methods. *Journal of Neuroscience*, 28(8):1929–1942, feb 2008.
- [23] Mads Dyrholm, Christoforos Christoforou, and Lucas C Parra. Bilinear Discriminant Component Analysis. *The Journal of Machine Learning Research*, 8:1097–1111, 2007.
- [24] Byron M. Yu, Jp Cunningham, Gopal Santhanam, Si Ryu, Krishna V. Shenoy, and Maneesh Sahani. Gaussian-Process Factor Analysis for Low-Dimensional Single-Trial Analysis of Neural Population Activity. *Journal of Neurophysiology*, 102(April 2009):614–635, 2009.
- [25] Yuan Zhao and II Memming Park. Variational Latent Gaussian Process for Recovering Single-Trial Dynamics from Population Spike Trains. *Neural Computation*, 29(5):1293–1316, may 2017.
- [26] Jessica K. Nadalin, Louis Emmanuel Martinet, Ethan B. Blackwood, Meng Chen Lo, Alik S. Widge, Sydney S. Cash, Uri T. Eden, and Mark A. Kramer. A statistical framework to assess cross-frequency coupling while accounting for confounding analysis effects. *eLife*, 8, oct 2019.
- [27] Benedikt V Ehinger and Olaf Dimigen. Unfold: An integrated toolbox for overlap correction, non-linear modeling, and regression-based EEG analysis. *bioRxiv*, page 360156, dec 2018.

Appendix A Identifiability, constraints and offsets

One solution to the identifiability problem is to constrain all functions to take be null at some value and add offsets c_{ij} . We still need to had further constraints on the offset depending on the structure of the model:

- We impose $c_{ij} = 1$ for $j > 1$. This avoids equivalent models by scaling all $f_{k(ij1)}$ and c_{i1} by λ , and all $f_{k(ijl)}$ and c_{ij} by $1/\lambda$.
- If there is any fixed function in factor j , i.e if there is one $f_{k(ijl)} = h_{k(ijl)}$, then the offset is not needed because setting the value of this function removes the scaling equivalency. Therefore we set $c_{ij} = 0$, and remove all constraints on functions in factor j .
- we also impose $c_{i1} = 0$ if $D_i = 1$. If there is no interaction terms for block i , as in a standard GAM, then we need to remove the equivalence between parameters c_{1i} and c_0 .

Provided the constraints above, our model will be identifiable, unless there is a null factor, i.e. unless there is (i, j) where $\sum_l f_{k(ijl)}(x) = 0$ for all $x \in \mathcal{X}$. Note that it is also possible, when offset c_{ij} is not constrained, to absorb it into one of the functions in the factor (and remove the constraint on that function). For example instead of $f_1(x) + f_2(x) + c$ with a constraint on f_1 and f_2 , we can use equivalently $f_1(x) + f_2(x)$ with a constraint on f_2 only.

The form of the constraint on each f does not necessarily have to be that $f(x_0) = 0$ for a given x_0 . A different constraint may be used to facilitate the interpretations of the results. For example, in the experimental analysis of Figure 6, we chose a constraint that the average of the weights w_k be 1. In general, we will use linear constraints on function evaluations $\mathbf{p}_k^T \mathbf{f}_k = l_k$. By identifying an orthonormal basis \mathbf{P}_k for the subspace of \mathbb{R}^V that is orthogonal to \mathbf{p}_k , we project \mathbf{f}_k onto this subspace and obtain free parameters $\tilde{\boldsymbol{\theta}}_k = \mathbf{P}_k \mathbf{f}_k \sim \mathcal{N}(\mathbf{P}_k \boldsymbol{\mu}_k, \mathbf{P}_k \mathbf{K}_k \mathbf{P}_k^T)$, such that $\mathbf{f}_k = \mathbf{p}_k l_k + \mathbf{P}_k^T \tilde{\boldsymbol{\theta}}_k$. If there is no constraint on a set of weights we simply have $\mathbf{P}_k = \mathbf{I}$ and $l_k = 0$. In practice we will use four types of constraint:

1. *first-zero constraint*, i.e. $f_k(x_0) = 0$, is the default constraint that the function must be null at some defined value x_0 . The projection matrix \mathbf{P}_k is simply the identity matrix deprived of the corresponding line.
2. *mean-zero constraint*, i.e. $\sum_n f_k(n) = 0$. This corresponds to $l_k = 0$ and corresponding projection matrix $P_k(m, n) = \frac{1}{\sqrt{m(m+1)}}$ if $m \geq n$, $P_k(m, m+1) = -\frac{m}{\sqrt{m(m+1)}}$ and $P_k(m, n) = 0$ if $m < n$. This constraint is useful in the GAM context, i.e. when the activations are taken as the sums of GPs $\rho(x) = \sum_k f_k(x_k)$. In GUMs, we will generally impose mean-zero constraint for all but one functions inserted in one-dimensional components.
3. *mean-one constraint*, i.e. $\sum_n f_k(n) = l_k = 1$ (the projection matrix is same as for mean-zero constraint). This is equivalent to mean-zero constraint and absorbing offset $c = 1$.
4. *sum-one constraint*, i.e. $\sum_n f_k(n) = V_k$, is an alternative to mean-one constraint.

Appendix B Laplace approximation for GUM

B.1 Conversion to GMM with Gaussian prior

The parameters to infer are $\boldsymbol{\theta} = \{\mathbf{f}_{1..K}, \mathbf{c}\}$, where $\mathbf{f}_k = f_k(\mathbf{x}_k)$ and \mathbf{x}_k the vector of v_k unique values taken by $x_{s(k)}$ in the dataset. f_k have MVN prior $\mathcal{N}(\boldsymbol{\mu}_k, \mathbf{K}_k)$ and each offset parameter has normal prior $\mathcal{N}(0, \sigma^2)$, so $\boldsymbol{\theta}$ has MVN prior with mean $(\boldsymbol{\mu}_1, \dots, \boldsymbol{\mu}_K, \mathbf{0})$ and a block-diagonal covariance matrix. Instead of fully flexible functions f_k , we can also impose linearity, i.e. $f_k(\mathbf{x}) = \mathbf{w}_k^T \mathbf{x}_{s(k)}$. In this case, we define an isometric MVN prior on the weights (akin to L2-regularization), i.e. $\mathbf{f}_k = \mathbf{w}_k$ and $\mathbf{f}_k \sim \mathcal{N}(\mathbf{0}, \sigma_k^2 \mathbf{I})$.

We can write $f_k(\mathbf{x}^{(n)}) = \boldsymbol{\Phi}_{kn} \cdot \boldsymbol{\theta}$ where $\boldsymbol{\Phi}_{kn}$ is an indicator vector of length v_k whose value 1 indicates the position of the corresponding parameter in the parameter set. If function f_k decomposes as the product of a fixed function h_k and function to be estimated \tilde{f}_k , then parameters are $\mathbf{f}_k = \tilde{f}_k(\mathbf{x})$ and the values of $\boldsymbol{\Phi}_{kn}$ are changed to $h_k(\mathbf{x}^{(n)})$. In the case of linear mapping, we have $\boldsymbol{\Phi}_k = (\mathbf{x}_{s(k)})$ (i.e. the classical design matrix of a GLM). Finally a fixed function $f_k = h_k$ has no parameter.

The values taken by factor $F_{ij}(\mathbf{x}) = \sum_l f_{k(ijl)}(\mathbf{x})$ in the dataset is $\mathbf{F}_{ij} = F_{ij}(\mathbf{X}) = \boldsymbol{\Phi}_{ij} \boldsymbol{\theta}_{ij} + \mathbf{C}_{ij}$, where $\boldsymbol{\theta}_{ij}$ is the subset of $\boldsymbol{\theta}$ that parametrises factor F_{ij} , the design matrix $\boldsymbol{\Phi}_{ij}$ for factor F_{ij} is built by concatenating design matrices $\boldsymbol{\Phi}_{k(ijl)}$ for individual functions, and including also the term for dependence in offset c_{ij} if it is a free parameter. \mathbf{C}_{ij} sums all fixed values, i.e. h_k for fixed functions f_k in the factor, and c_{ij} if its value is fixed.

Now we see that the equation of a GUM (equation 1) can be replaced with a generalized multilinear model [11, 22] with C blocks and Gaussian priors for the weights:

$$\boldsymbol{\rho} = \sum_{i=1}^C \prod_{j=1}^{D_i} (\boldsymbol{\Phi}_{ij} \boldsymbol{\theta}_{ij}^T + \mathbf{C}_{ij}) \quad (6)$$

B.2 Maximum A Posteriori weights

To identify the Maximum A Posteriori solution, we use the general solution for generalized multilinear models which is to optimise over set of parameters in one factor while keeping others factors in the block constant, pass on the next factor and iterate until convergence ([22]). At each iteration, we optimise weights over factor j_i^* for each block i . The optimization is possible as long as the parameters $\boldsymbol{\theta}_{ij}$ in the factors are not also present in the factors that are fixed, i.e. if there are no calls to the same function in the different factors of the same block (the method cannot be applied to model $\rho(\mathbf{x}) = f_1(\mathbf{x})(f_1(\mathbf{x}) + f_2(\mathbf{x}))$). However it is perfectly possible to have different calls to the same function in different blocks, for example defining $\rho(\mathbf{x}) = f_1(x_1)f_2(x_2) + f_1(x_3)f_4(x_4)$.

The generative model transforms to :

$$\begin{cases} \boldsymbol{\rho} &= \sum_i (\boldsymbol{\Phi}_{(i, \neg j_i^*)} \boldsymbol{\theta}_{i, j_i^*} + \mathbf{C}_{i, j_i^*}) \\ &= \sum_i \boldsymbol{\Phi}_{(i, \neg j_i^*)} \mathbf{P}_{i, j_i^*}^T \tilde{\boldsymbol{\theta}}_{i, j_i^*} + \mathbf{C}^*, \text{ where} \\ \mathbf{C}^* &= \sum_i (\mathbf{C}_{i, j_i^*} + \mathbf{P}_{i, j_i^*} \boldsymbol{\Phi}_{(i, \neg j_i^*)} \mathbf{P}_{i, j_i^*}^T) \end{cases} \quad (7)$$

where the new covariates are obtained by collapsing over fixed factors $j \neq j_i^*$: $\boldsymbol{\Phi}_{(i, \neg j_i^*)} = \prod_{j \neq j_i^*} (\boldsymbol{\Phi}_{ij} \boldsymbol{\theta}_{ij}^T + \mathbf{C}_{ij})$. We see that the predictor is linear with respect to the set of weights $\tilde{\boldsymbol{\theta}}$ corresponding to all $\tilde{\boldsymbol{\theta}}_{i, j_i^*}$ in all blocks i . We thus obtain the generative equation from a GLM with MVN prior:

$$g(\mathbb{E}(y^{(n)})) = \boldsymbol{\rho} = \tilde{\boldsymbol{\Phi}}^* \tilde{\boldsymbol{\theta}}^{*T} + \mathbf{C}^* \quad (8)$$

$$\text{where } \tilde{\boldsymbol{\Phi}}^* = \boldsymbol{\Phi}^* \mathbf{P}^{*T}, \boldsymbol{\Phi}_n^* = [\boldsymbol{\Phi}_{(1, \neg j_1^*)} \cdots \boldsymbol{\Phi}_{(C, \neg j_C^*)}] \text{ and } \mathbf{P}^* = \begin{bmatrix} \mathbf{P}_{(1, j_1^*)} \\ \cdots \\ \mathbf{P}_{(C, j_C^*)} \end{bmatrix}$$

We update the set of weights $\tilde{\boldsymbol{\theta}}^*$ with a single Newton-Raphson update. Prior mean for $\tilde{\boldsymbol{\theta}}^*$ is MVN, with means $\boldsymbol{\mu}^*$ and covariance \mathbf{K}^* extracted from the $\boldsymbol{\mu}$ and \mathbf{K} . The log-posterior over $\tilde{\boldsymbol{\theta}}^*$ can be expressed as:

$$\begin{cases} \log p(\tilde{\boldsymbol{\theta}}^* | \mathbf{y}) &= \log(\mathbf{y} | \tilde{\boldsymbol{\theta}}^*) + \log p(\tilde{\boldsymbol{\theta}}^*) + \text{const} \\ &= \frac{1}{s} \sum_{n=1}^N (\eta_n y^{(n)} - B(\eta_n)) - \frac{1}{2} ((\tilde{\boldsymbol{\theta}}^* - \tilde{\boldsymbol{\mu}}^*)^T (\mathbf{K}^*)^{-1} (\tilde{\boldsymbol{\theta}}^* - \tilde{\boldsymbol{\mu}}^*)) + \text{const} \end{cases} \quad (9)$$

where η_n and s are respectively the canonical and dispersion parameter of the exponential family distribution for y_n , and $B(\eta_n)$ is such that $\frac{dB}{d\eta} = \mathbb{E}(y^{(n)}) = g^{-1}(\rho_n)$. In the following we assume that g is the canonical link function (similar updates can be found in the general case).

Since the gradient of $\rho^{(n)}$ w.r.t weights $\tilde{\boldsymbol{\theta}}^*$ is $\tilde{\boldsymbol{\Phi}}_n^* \mathbf{P}^*$, the gradient and Hessian of the log-posterior gives:

$$\begin{cases} \nabla \log p(\tilde{\boldsymbol{\theta}}^* | \mathbf{y}) &= \frac{1}{s} \sum_{n=1}^N \tilde{\boldsymbol{\Phi}}_n^{*T} (y^{(n)} - g^{-1}(\rho_n)) - (\mathbf{K}^*)^{-1} (\tilde{\boldsymbol{\theta}}^* - \tilde{\boldsymbol{\mu}}^*) \\ \nabla \nabla \log p(\tilde{\boldsymbol{\theta}}^* | \mathbf{y}) &= -\frac{1}{s} \sum_{n=1}^N \tilde{\boldsymbol{\Phi}}_n^{*T} R_{nn} \tilde{\boldsymbol{\Phi}}_n^* - (\mathbf{K}^*)^{-1} \end{cases} \quad (10)$$

\mathbf{R} is a diagonal matrix such that $R_{nn} = (g^{-1})'(\rho^{(n)}) = \frac{1}{g'(g^{-1}(\rho^{(n)}))}$.

The Newton-Raphson update gives:

$$\begin{cases} \tilde{\boldsymbol{\theta}}_{\text{new}}^* &= \tilde{\boldsymbol{\theta}}^* - (\nabla \nabla \log p(\tilde{\boldsymbol{\theta}}^* | \mathbf{y}))^{-1} \nabla \log p(\tilde{\boldsymbol{\theta}}^* | \mathbf{y}) \\ &= \tilde{\boldsymbol{\theta}}^* + (\mathbf{K}^* \tilde{\boldsymbol{\Phi}}^{*T} \mathbf{R} \tilde{\boldsymbol{\Phi}}^* + s \mathbf{I})^{-1} (\mathbf{K}^* \tilde{\boldsymbol{\Phi}}^{*T} (\mathbf{y} - g^{-1}(\boldsymbol{\rho})) - s(\tilde{\boldsymbol{\theta}}^* - \tilde{\boldsymbol{\mu}}^*)) \\ &= \mathbf{H}^{-1} \mathbf{B} \text{ with} \\ \mathbf{H} &= \mathbf{K}^* \tilde{\boldsymbol{\Phi}}^{*T} \mathbf{R} \tilde{\boldsymbol{\Phi}}^* + s \mathbf{I} \\ \mathbf{B} &= \mathbf{K}^* \tilde{\boldsymbol{\Phi}}^{*T} (\mathbf{R} \tilde{\boldsymbol{\rho}} + \mathbf{y} - g^{-1}(\boldsymbol{\rho})) + s \tilde{\boldsymbol{\mu}}^* \end{cases} \quad (11)$$

We have defined $\tilde{\rho} = \tilde{\Phi}^* \mathbf{P}^* \tilde{\theta}^* = \rho - \mathbf{C}^*$. From equation (11) we obtain the new values for all weights $\theta_{(i,j_i^*)}$. The algorithm loops by selecting at each iteration a new set of factors j_i^* and then applying equations (7,8, 11) to update the values of $\theta_{(i,j_i^*)}$.

If there are several set of unconstrained weights in the same block, convergence may take many iterations as the scaling of the weights are only constrained by the different priors. In such cases, it is convenient to re-scale these set of weights after each iteration to speed up convergence time:

$$\theta_{ij}^{\text{new}} = \frac{(\prod_{j'} \alpha_{ij'})^{\frac{1}{2D_i^{\text{free}}}}}{\sqrt{\alpha_{ij}}} \theta_{ij}, \text{ with } \alpha_{ij} = (\theta_{ij} - \mathbf{P}_{ij})^T (\mathbf{K}_{ij})^{-1} (\theta_{ij} - v\mathbf{K}_{ij})^T \quad (12)$$

The product is taken over all free constraint dimensions in the component (D_i^{free} is the number of such dimensions).

B.3 Posterior covariance

In the Laplace approximation, the posterior mean is provided by the MAP weights while the posterior covariance for weights is approximated from the full Hessian of the log-posterior. Hessian for free weights in the same set (same component, same dimension) are provided by equation 11. For free weights in different sets θ_{ij} and $\theta_{(i',j')}$, we have:

$$\nabla_{\tilde{\theta}_{ij}} \nabla_{\tilde{\theta}_{i'j'}} \log p(\tilde{\theta}|\mathbf{y}) = (\Phi_{(i,\neg j)})^T \mathbf{R} \Phi_{(i',\neg j')} \quad (13)$$

Once we have identified the approximate posterior covariance for free parameters $\tilde{\Sigma} = -(\nabla_{\tilde{\theta}} \nabla_{\tilde{\theta}} \log p(\tilde{\theta}|\mathbf{y}))^{-1}$, we recover the posterior for parameters θ which is $\Sigma = \mathbf{P}^T \tilde{\Sigma} \mathbf{P}$ (matrix \mathbf{P} is block diagonal formed with all \mathbf{P}_k for all components and dimensions).

The Laplace approximation can be used to generate predictions for $f_k(x')$ at values of x' not included in the training set ([4]):

$$\begin{cases} f_k(x') &= \mathcal{N}(m', (v')^2), \text{ where} \\ m' &= K_k(x', \mathbf{x}_k) (\mathbf{K}_k)^{-1} \mathbf{f}_k^{\text{MAP}} \\ (v')^2 &= K_k(x', x') - K_k(x', \mathbf{x}_k)^T (\Sigma_k)^{-1} K_k(x', \mathbf{x}_k) \end{cases} \quad (14)$$

The Laplace approximation can also be used to approximate the log-marginal evidence $p(\mathbf{y})$ ([4]):

$$\log p(\mathbf{y}|\mathbf{X}) \approx -\frac{1}{2} (\tilde{\theta}^{\text{MAP}} - \tilde{\mu})^T \tilde{\mathbf{K}}^{-1} (\tilde{\theta}^{\text{MAP}} - \tilde{\mu}) + \log p(\mathbf{y}|\mathbf{X}, \tilde{\theta}^{\text{MAP}}) - \frac{1}{2} \log |\mathbf{I} + \frac{1}{2} \tilde{\mathbf{K}} \mathbf{W}| \quad (15)$$

B.4 Hyperparameter fitting

B.4.1 Maximising cross-validated score

Here, we first find MAP values $\tilde{\theta}^{\text{MAP}}$ from a training set (\mathbf{x}, \mathbf{y}) and compute a fitting score for $\tilde{\theta}^{\text{MAP}} = \arg \max p(\tilde{\theta}|\mathbf{x}, \mathbf{y}, \gamma)$ on a cross-validation set $(\mathbf{X}', \mathbf{y}')$. We wish to find hyperparameters γ that maximises the cross-validated score $S(\tilde{\theta}; \mathbf{X}', \mathbf{y}')$. Here we will use the log-likelihood as the score, i.e. $S(\tilde{\theta}; \mathbf{X}', \mathbf{y}') = \log(\mathbf{y}'|\mathbf{X}', \tilde{\theta})$. The gradient of the score w.r.t to hyperparameters can be computed using the chain rule:

$$\begin{cases} \nabla_{\gamma} S(\tilde{\theta}^{\text{MAP}}; \mathbf{X}', \mathbf{y}') &= \nabla_{\gamma} \tilde{\theta}^{\text{MAP}} \cdot \nabla_{\tilde{\theta}} S(\tilde{\theta}^{\text{MAP}}; \mathbf{X}', \mathbf{y}') \\ &= \frac{1}{s} \nabla_{\gamma} \tilde{\theta}^{\text{MAP}} \cdot \mathbf{P} \sum_{k=1}^{n'} (y_{k'} - g^{-1}(a_{k'})) \nabla_{\mathbf{U}} a_{k'} \end{cases} \quad (16)$$

From equation 7, we can see that the gradient of $a_{k'}$ is obtained by concatenating pseudo-design matrices $(\Phi_{\cdot k'}^{(1,-1)}, \dots, \Phi_{\cdot k'}^{(C,-D_C)})$. From the definition of the MAP weights $\tilde{\theta}^{\text{MAP}}$, the Jacobian with respect to hyperparameters is:

$$\begin{cases} \nabla_{\gamma} \tilde{\theta}^{\text{MAP}} &= -H^{-1} (\nabla_{\gamma} \nabla_{\tilde{\theta}} \log p(\tilde{\theta}^{\text{MAP}}|\mathbf{X}, \mathbf{y}, \gamma)) \\ &= -H^{-1} \mathbf{P} (\nabla_{\gamma} \nabla_{\mathbf{U}} \log \mathcal{N}(\tilde{\theta}^{\text{MAP}}; \mathbf{0}, \mathbf{K}(\gamma))) \\ &= -H^{-1} \mathbf{P} \mathbf{K}^{-1} \nabla_{\gamma} \mathbf{K} \mathbf{K}^{-1} \tilde{\theta}^{\text{MAP}} \end{cases} \quad (17)$$

where $H = (\nabla_{\tilde{\theta}} \nabla_{\tilde{\theta}} \log p(\tilde{\theta}^{\text{MAP}} | \mathbf{X}, \mathbf{y}, \gamma))$ and we have omitted the dependence of the covariance prior on the hyperparameters $\mathbf{K} = \mathbf{K}(\gamma)$. Instead of maximising the cross-validated score on a single cross-validation set, the score (and its gradient) can be averaged over multiple partitions of the data into training and cross-validation sets for more robust results. In many situations, the GP covariance K will be close to singularity so $\mathbf{K}^{-1} \nabla_{\gamma} \mathbf{K} \mathbf{K}^{-1}$ may be subject to large numerical errors. In such case, the gradient of the score cannot be evaluated properly, so maximization of the score should use gradient-free optimization procedure such as simplex algorithms.

B.4.2 Maximise marginal likelihood through Expectation-Maximisation

An alternative way of fitting the hyperparameters is to maximise the marginal likelihood $p(\mathbf{y} | \mathbf{X}, \gamma) = \int p(\mathbf{y} | \mathbf{X}, \tilde{\theta}) p(\tilde{\theta} | \gamma) d\tilde{\theta}$ through Expectation-Maximisation. In the E-step we use the Laplace approximation to derive an approximate posterior for the weights $p(\tilde{\theta} | \mathbf{X}, \gamma) \approx q(\tilde{\theta}) = \mathcal{N}(\tilde{\theta}^{\text{MAP}}, \tilde{\Sigma})$. In the M-step we maximise the lower bound w.r.t to hyperparameters (which define covariance matrices \mathbf{K}_{ij}):

$$\left\{ \begin{array}{l} Q(\gamma) = \int p(\tilde{\theta} | \mathbf{X}, \gamma_{\text{old}}) \log p(\mathbf{X}, \tilde{\theta} | \gamma) d\tilde{\theta} \\ \approx \int \mathcal{N}(\tilde{\theta}^{\text{MAP}}, \tilde{\Sigma}) \log \mathcal{N}(\tilde{\theta}; \mathbf{P}, \mathbf{K}) d\tilde{\theta} + \text{const} \\ \approx \frac{1}{2} \text{Tr}((\mathbf{P} \mathbf{K} \mathbf{P}^T)^{-1} \tilde{\Sigma}) + \frac{1}{2} \log \det(\mathbf{P} \mathbf{K} \mathbf{P}^T) \\ \quad + \frac{1}{2} (\tilde{\theta}^{\text{MAP}} - \mathbf{P} \mathbf{P})^T (\mathbf{P} \mathbf{K} \mathbf{P}^T)^{-1} (\tilde{\theta}^{\text{MAP}} - \mathbf{P} \mathbf{P}) + \text{const} \\ \approx \frac{1}{2} \sum_k [\text{Tr}((\mathbf{P}_k \mathbf{K}_k \mathbf{P}_k^T)^{-1} \tilde{\Sigma}_k) + \log \det(\mathbf{P}_k \mathbf{K}_k \mathbf{P}_k^T) \\ \quad + (\tilde{\theta}_k^{\text{MAP}} - \mathbf{P}_k \boldsymbol{\mu}_{ij})^T (\mathbf{P}_k \mathbf{K}_k \mathbf{P}_k^T)^{-1} (\tilde{\theta}_k^{\text{MAP}} - \mathbf{P}_k \boldsymbol{\mu}_k)] + \text{const} \end{array} \right. \quad (18)$$

The hyperparameters related to each dimension of each component γ_k can be optimised independently by maximising the related quantity in the sum of equation 18 through gradient search. In the case of L2-regularization ($\boldsymbol{\mu}_k = \mathbf{0}$ and $\mathbf{K}_k = \lambda_k^2 \mathbf{I}$), we can get the analytical solution [3]:

$$\lambda_k^2 = \frac{\|\tilde{\theta}_k\|^2 + \text{Tr}(\tilde{\Sigma}_k)}{\text{card}(k)} \quad (19)$$

Appendix C Estimation error on synthetic dataset

We measured the estimation error of GUM in different ways. First, we measured the mean square error of estimated predictor $\frac{1}{n} \sum_n (\hat{\rho}^{(n)} - \rho_{\text{true}}^{(n)})^2$. Since GUM is essentially an inference tool, where the principal interest is about inferring function f_k , we can also compute the error on these function. We defined the estimation error on the function $\text{err}(f)$ as the expected mean square error over function evaluation under the posterior distribution over the function, i.e. $\text{err}(f_k) = \frac{1}{n} \sum_n \int (f_k^{(n)} - f_{k,\text{true}}^{(n)})^2 p(f_k^{(n)} | \mathbf{y}) df_k^{(n)}$. The error decomposes into a bias term (the mean squared error for the posterior mean), and a variance term (the mean variance of the posterior at evaluated points):

$$\left\{ \begin{array}{l} \text{err}(f_k) = \frac{1}{n} \sum_n \int ((f - \mu_k^{(n)}) - (f_{k,\text{true}} - \mu_k^{(n)}))^2 \mathcal{N}(f; \mu_k^{(n)}, \sigma_k^{(n)2}) df \\ = \frac{1}{n} \sum_n [(f_{k,\text{true}} - \mu_k^{(n)})^2 + (f - \mu_k^{(n)})^2 \\ \quad - 2(f - \mu_k^{(n)})(f_{k,\text{true}} - \mu_k^{(n)})] \mathcal{N}(f; \mu_k^{(n)}, \sigma_k^{(n)2}) df \\ = \frac{1}{n} \sum_n (f_{k,\text{true}} - \mu_k^{(n)})^2 + \frac{1}{n} \sum_n \sigma_k^{(n)2} \end{array} \right. \quad (20)$$

Appendix D Experimental procedure

Each stimulus sequence consisted of five to ten gratings. Each grating was a high-contrast Gabor patch (colour: blue or purple; spatial frequency = 2 cycles per degree; SD of Gaussian envelope = 1 degree) presented within a circular aperture (4 degrees) against a uniform gray background. Each grating was presented during 100 ms, and the interval between gratings was fixed to 300 ms. The angles of the gratings were sampled from a von Mises distribution centered on the reference angle (45 degrees for category associated with right response, 135 degrees for category associated with left response) and with concentration coefficient $\kappa = 0.3$. Each sequence was preceded by a rectangle flashed twice during 100 ms (the interval between the flashes and between the second flash and the first grating varied between 300 and 400 ms). Participant indicated their choice with a button press after the onset of a centrally occurring dot that

succeeded the backward mask and were made with a button press with the right hand. Failure to provide a response within 1000 ms after central dot onset was classified as invalid trial. Auditory feedback was provided 250 ms after participant response (at latest 1100 ms after end of stimulus sequence). It consisted of an ascending tone (400 Hz/800 Hz; 83 ms/167 ms) for correct responses; descending tone (400 Hz/ 400 Hz; 83 ms/167 ms) for incorrect responses; a low tone (400 Hz; 250 ms) for invalid trials. Trials were separated by a blank interstimulus interval of 1,200-1,600 ms (truncated exponential distribution of mean 1,333 ms). Experiments consisted of 480 trials in 10 blocks of 48. It was preceded with two blocks of initiation with 36 trials each. In the first initiation block, there was only one grating in the sequence, and it was perfectly aligned with one of the reference angles. In the second initiation block, sequences of gratings were introduced, and the difficulty was gradually increased (the distribution concentration linearly decreased from $\kappa = 1.2$ to $\kappa = 0.3$). Invalid trials (mean 6.9 per participant, std 9.4) were excluded from all regression analyses.

Visual stimuli were generated and behavioral responses recorded using Psychophysics-3 Toolbox in addition to custom scripts written for Matlab (MathWorks).